Molecular Ecology

WILEY

MOLECULAR ECOLOGY

ORIGINAL ARTICLE

The Insurgence of Strong Hybrid Seed Inviability Explains the Initial Phases of Divergence in the Rapidly Evolving *Dianthus rupicola* Complex

Lucrezia Laccetti[1] | Donata Cafasso[1] | Teresa R. Galise[1] | Antonia Cristaudo[2] | Bárbara S. Santos Leal[3,4] | João Pedro S. Pena Bento[3] | Juliana L. Sampaio Mayer[3] | Fabio Pinheiro[3] | Giovanni Scopece[1]

[1]Department of Biology, University of Naples Federico II, Naples, Italy | [2]Department of Biological, Geological and Environmental Sciences, University of Catania, Catania, Italy | [3]Departamento de Biologia Vegetal, Instituto de Biologia, Universidade Estadual de Campinas, Campinas, Brazil | [4]Instituto Tecnológico Vale, Belém, Brazil

Correspondence: Lucrezia Laccetti (lucrezia.laccetti@unina.it) | Giovanni Scopece (giovanni.scopece@unina.it)

Received: 14 January 2026 | **Revised:** 12 May 2026 | **Accepted:** 15 May 2026

Keywords: endosperm balance number | evolutionary radiations | hybrid seed inviability | postzygotic barriers

ABSTRACT

Understanding the mechanisms underlying fast diversifications is central to evolutionary biology. This can be partly achieved by focusing on intrinsic reproductive barriers that emerge during early stages of divergence in fast-radiating groups. Here, we explored the mechanisms underlying the divergence of two ecotypes of the *Dianthus rupicola* complex, which belong to the Eurasian clade of the hyperdiverse genus *Dianthus*, the fastest reported radiation among angiosperms. We combined phenotypic and genomic analyses, reciprocal crosses, and micromorphological observations at different stages of seed development (i.e., 3, 6, and 9 days after pollination) to discover putative reproductive barriers between these ecotypes. Our findings indicate that the ecotypes started diverging approximately 87 kya and rapidly developed strong hybrid seed inviability. Consistent with a divergence in Endosperm Balance Number (EBN) between the ecotypes, we observed a parent-of-origin growth effect on hybrid seeds which led to asymmetric seed size in reciprocal crosses. Genomic analyses revealed low levels of admixture between the two ecotypes despite their recent origin, consistent with the presence of strong intrinsic barriers to gene flow. This admixture was explained by past introgression rather than recent hybridization between the ecotypes. Overall, our study highlights the primary role of hybrid seed inviability in maintaining reproductive isolation in a rapid evolutionary radiation. Moreover, it opens new avenues for dissecting the molecular basis and the eventual ecological drivers of endosperm-mediated incompatibilities, as well as their largely unexplored yet potentially decisive contribution to diversification at short evolutionary timescales.

1 | Introduction

Understanding ecological and intrinsic mechanisms underlying fast diversifications is an important goal for evolutionary biologists, because it can expand our knowledge on the ultimate drivers of plant biodiversity (e.g., Givnish et al. 2015; Lagomarsino et al. 2016; Kong et al. 2022). This goal can be partly achieved by focusing on reproductive barriers between lineages that are in the first phase of divergence, that is, between different ecotypes of the same species, assuming that the mechanisms identified can then be used to test for more general hypotheses (Scopece et al. 2010; Lowry and Gould 2016; Butlin and Faria 2024). Similar studies have been conducted in several fast evolving plant groups and have generally emphasized the role of the rapid insurgence of prezygotic barriers, such as ecological isolation (e.g., pollinators, lifestyle; Givnish et al. 2015; Christie et al. 2022), ecogeographic isolation (Sobel 2014; Weng et al. 2023), and postmating prezygotic

barriers (pollen-stigma incompatibility; Bedinger et al. 2011; Suni and Hopkins 2018). These barriers, often controlled by a small number of genes with large effects, can evolve rapidly (e.g., Sedeek et al. 2014) and thereby contribute to fast diversification. Polyploidy has also been recognized as a mechanism capable of generating instantaneous postzygotic reproductive isolation and promoting rapid lineage formation (e.g., Balao et al. 2010). In contrast, postzygotic barriers between homoploid taxa are generally viewed as a byproduct of accumulated genetic divergence and thus are expected to require longer times to evolve (Moyle et al. 2004), making them less likely to explain rapid radiations. Nevertheless, recent evidence suggests that certain postzygotic barriers, such as hybrid seed inviability, can also arise quickly and may play an important role in early stages of diversification (Zeh and Zeh 2000; Gutierrez-Marcos et al. 2003; Coughlan 2023).

Hybrid seed inviability arises when fertilization successfully occurs, but the resulting seeds fail to develop properly (Queller 1983; Haig and Westoby 1989; Lafon-Placette and Köhler 2016; Coughlan 2023). A common conceptual framework to investigate hybrid seed inviability is the Endosperm Balance Number (EBN) theory (Johnston et al. 1980; Johnston and Hanneman Jr 1982), which identifies endosperm developmental failure due to deviations from the canonical 2:1 maternal-to-paternal genomic ratio in the endosperm as the main driver of hybrid seed abortion (Johnston et al. 1980; Bushell et al. 2003; Lafon-Placette and Köhler 2016; Coughlan 2023). This mechanism, typically associated with asymmetric seed development indicative of maternal or paternal excess (Scott et al. 1998; Briscoe Runquist et al. 2014; Lafon-Placette et al. 2018; Butel et al. 2024; Dziasek et al. 2024), is emerging as an important reproductive isolating mechanism in a growing number of angiosperm groups, but its role in fast evolutionary radiations is still unclear (but see Briscoe Runquist et al. 2014; Oneal et al. 2016; İltaş et al. 2021) and requires more evidence to support.

Among flowering plants, the Euroasiatic clade within the genus *Dianthus* experienced the most rapid diversification rate ever reported (Valente et al. 2010). This clade contains large numbers of narrow endemics (i.e., over 50% of European *Dianthus* taxa are narrow endemics) with small and geographically restricted ranges, typically associated with the pronounced topographic heterogeneity of the Mediterranean basin (e.g., Bittrich 1993; Fassou et al. 2022). Notably, a surprising bias in the literature regards the evolution of intrinsic reproductive barriers among this vast plethora of recently evolved endemic taxa. This literature bias is even more surprising considering that the first experimental interspecific cross ever conducted on plants was carried out between two *Dianthus* species in 1717 to intentionally produce a hybrid, the so-called "Fairchild's Mule" (Leapman 2012) and that, since then, an impressive amount of crossing combinations have been tested in the genus to produce hybrids with aesthetic and economic value (Katoch et al. 2024). These data on interspecific manual crosses, often showing abnormal development of embryos in hybrid seeds, however, never crossed the borders between horticultural and evolutionary biology research. Nevertheless, the evolution of intrinsic reproductive isolation is an important topic that would help understanding either the mechanisms limiting gene flow at the beginning of the speciation process or to predict the survival potential of the multitude of endemic *Dianthus* taxa in secondary contact, which is crucial under a climate change scenario (e.g., Gómez et al. 2015). The only study explicitly focusing on reproductive isolation between two *Dianthus* species, that is, *D. carthusianorum* and *D. sylvestris* identified pollinator isolation and extrinsic postzygotic isolation rather than postmating isolation as the main barriers (Cahenzli et al. 2018). However, these species are distantly related, thus making it difficult to elucidate which barriers played a key role at the initial phase of divergence.

In this study, with the aim of expanding our understanding on reproductive isolating mechanisms acting at the beginning of divergence in the fast-evolving Eurasiatic clade of *Dianthus* we focused on the *Dianthus rupicola* complex, a group that includes five geographically isolated and phenotypically differentiated diploid ecotypes (Domina et al. 2017). Specifically, we analysed 14 *D. rupicola* populations located in peninsular Southern Italy, Sicily, and Aeolian volcanic archipelago. These populations are traditionally assigned to either of two different subspecies/ecotypes, that is, *D. rupicola* subsp. *rupicola* (hereafter RUPI) and *D. rupicola* subsp. *aeolicus* (hereafter AEOL), based on vegetative and reproductive traits (Brullo and Minissale 2001; Domina et al. 2017). These populations share the same main pollinator (i.e., the hawk-moth *Macroglossum stellatarum*) and have very long and overlapping flowering periods (ranging from June to late October), indicating weak premating isolation (Laccetti et al. 2026). In these populations, we investigated genomic patterns and analysed putative mechanisms of postmating inter-ecotype reproductive isolation.

2 | Methods

2.1 | Study Species and Study System

Dianthus rupicola Biv. ($2n = 30$) is a chasmophyte, strictly related to cliff habitat and endemic to the Central Mediterranean, blooming from early summer to early autumn. Pink-purplish hermaphrodite flowers show proterandry and are grouped in inflorescences. The species is obligatory allogamous and the main pollinator is the hummingbird hawk-moth *Macroglossum stellatarum*, though other less abundant co-pollinators may also occur (Laccetti et al. 2026). Also, an antagonistic interaction with the pre-dispersal seed predator of the genus *Hadena* has been found to occur in RUPI but not in AEOL (Laccetti et al. 2026). Here, we investigated 14 populations located in peninsular Southern Italy, Sicily, and Aeolian Islands traditionally assigned to the two different ecotypes AEOL ($N_{population} = 7$) and RUPI ($N_{population} = 7$; see Figure 1 and Table S1). We collected seeds from each natural population at the end of the flowering season of 2020 and grew plants at the Department of Biology of the University of Naples Federico II (Italy) under the same environmental conditions. Seeds were obtained from at least 10 mother plants per population (inter-family distance ≥ 2 m) within an area of approximately 250 m^2. Seeds were kept separate by maternal family and germinated in greenhouses, leading to a total of 265 adult plants (N_{min} per population = 10, N_{max} per population = 20).

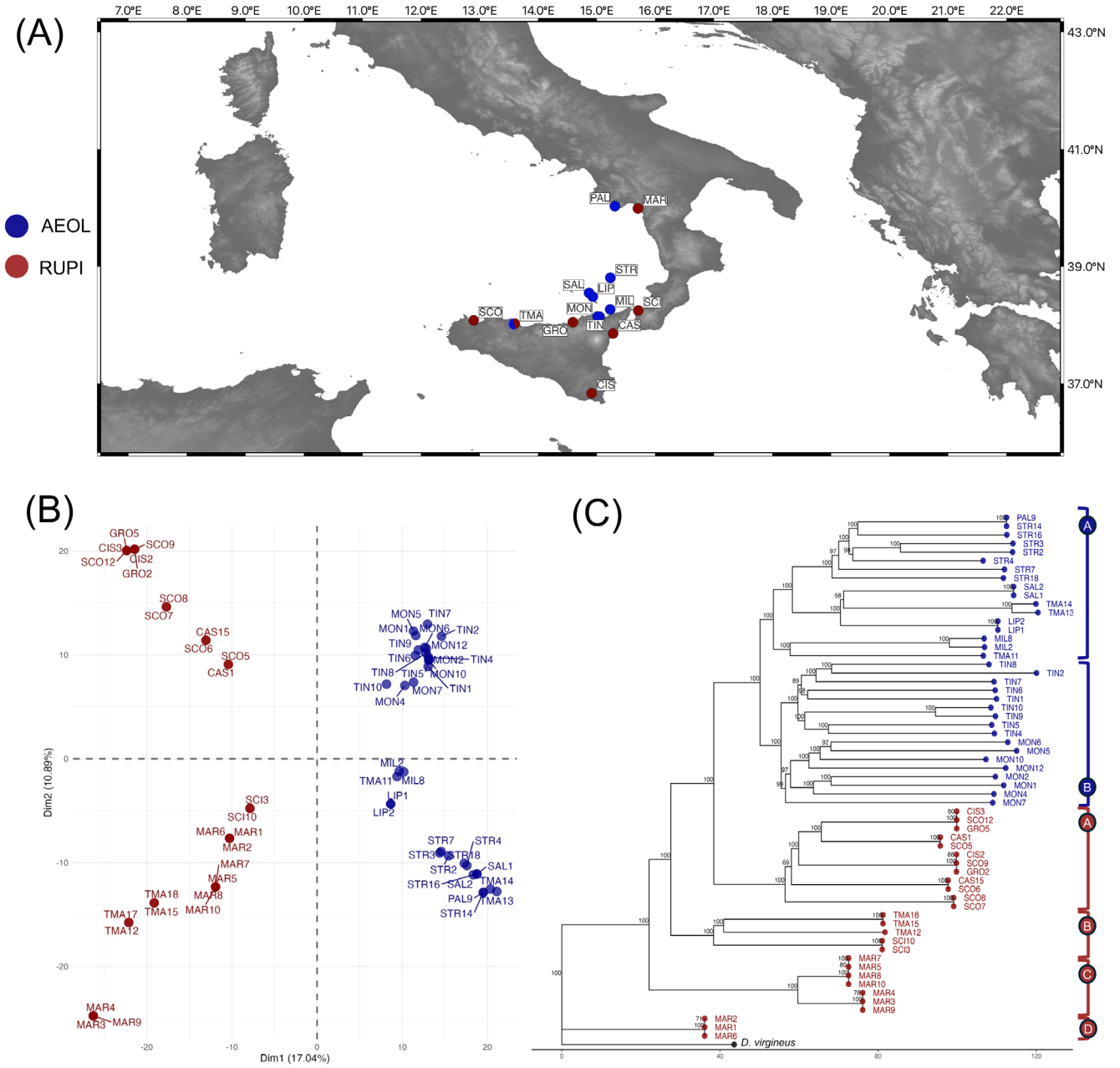

FIGURE 1 | Study system and genomic characterization of 14 *Dianthus rupicola* populations. Geographic distribution (A), genomic PCA (B) and neighbour-joining (NJ) tree (C) conducted on *Dianthus rupicola* populations. Blue denotes the *aeolicus* ecotype (AEOL), while red denotes the *rupicola* ecotype (RUPI). NJ shows populations from four clades of RUPI denoted by A, B, C and D, and two subclades of AEOL denoted by A and B, where A corresponds to the subclade including populations from Aeolian islands and coastal sites, while B corresponds to the subclade including Sicilian populations.

2.2 | Phenotypic Characterization

To examine population phenotypic divergence, we measured floral traits potentially attractive for pollinators and pre-dispersal seed predators in the common garden at the peak of the flowering period. We recorded the number of flowers per inflorescence on an average of 16 individuals per population, on 11 populations. Then, to account for variation within individuals, we collected 6 fully opened flowers (three flowers in the male phase and three flowers in the female phase) per individual ($N = 1044$ flowers). Each flower was photographed using a Sony alpha 65 digital camera and a millimetre scale as a reference. The software package Image J (https://imagej.nih.gov/ij/) was thus used to measure the following parameters: (1) style length, (2) calyx length, (3) petal length, (4) petal width, and (5) corolla diameter. Style length was determined as the distance from the nectary to the tip of the stigma.

2.3 | DNA Extractions, ddRAD Library Construction and Sequencing

We performed genomic analyses on 70 *D. rupicola* individuals belonging to the 14 investigated populations and one individual

of the *D. virgineus* complex collected in the TMA population. Following the protocol of the manufacturer, genomic DNAs were extracted from leaf material using the DNeasy Plant Mini Kit (Qiagen, Hilden, Germany). The quantity and the purity of DNA extractions were checked using the NanoDrop ND 1000 Spectrophotometer (Thermo Fisher Scientific, Delaware), whereas the concentration was assessed with the Qubit fluorometer system (Invitrogen, United States) and the Quant-IT ds-DNA BR Assay kit (Invitrogen). Samples were sequenced using the standard ddRAD protocol described in Peterson et al. (2012), with the restriction enzymes *Eco*RI and *Taq*I. A single library with barcoded individuals was sequenced in a single Illumina HiSeq 2500 lane for 150-base single-end reads. The demultiplexed, trimmed, and filtered reads were used as input for the software STACKS v2.4 (Rochette et al. 2019) in which the assembly was performed as described in Methods S1. Our filtering strategy resulted in a dataset of 21,935 biallelic SNPs across 62 individuals.

2.4 | Population Genetic Structure

To investigate the genetic structure of the sampled populations, we performed a Principal Component Analysis (PCA) as implemented in the *adegenet* package (Jombart 2008) in R 4.3.3 (R Core Team 2024). The first two PCs were visualized to assess the overall genomic structure and differentiation between ecotypes. Then, we built a neighbour-joining (NJ) tree by calculating pairwise Euclidean genetic distances between the 62 *D. rupicola* individuals and one individual of *D. virgineus* included as an outgroup in the *adegenet* package. To assess node support, we performed bootstrap resampling with 1000 replicates in the *ape* package (Paradis and Schliep 2019). The tree was visualized using the *ggtree* package (Yu et al. 2017). Lastly, to distinguish between recent hybridization or ancient introgression, we employed a two-step approach. First, individual admixture proportions were estimated using the sparse non-negative matrix factorization (sNMF) algorithm implemented in the *LEA* package (Frichot and François 2015). The sNMF method is computationally efficient and provides results comparable to STRUCTURE (Pritchard et al. 2000) without assuming Hardy–Weinberg equilibrium. We tested genetic clusters (K) ranging from 1 to 10, with 10 independent runs for each K value to assess convergence. The optimal K was determined by selecting the value with the lowest cross-entropy criterion (Frichot et al. 2014). Since continuous admixture coefficients can sometimes reflect shared ancestral variation rather than recent gene flow, we subsequently applied a discrete classification method using *Snapclust* implemented in the R package *adegenet* (Beugin et al. 2018). *Snapclust* assigns individuals to specific hybrid categories (F_1, F_2, Backcross) based on genotype likelihoods. Therefore, we explicitly tested for the presence of early hybrid classes by supplying hybridization coefficients for F_1 (0.5) and first-generation backcrosses (0.25). Finally, to provide a formal evaluation of introgression between the two ecotypes, including potentially older events not detectable by individual-assignment methods, we performed D-statistics (i.e., ABBA-BABA tests; Green et al. 2010) using a population-level frequency-based approach (Martin et al. 2015) as implemented in Dsuite (Malinsky et al. 2021). Following the phylogenetic structure inferred in our study, we defined the four-taxon arrangement as follows: P1 = AEOL (A), P2 = AEOL (B), P3 = RUPI (A; i.e., only the sister clade of AEOL), and O = *D. virgineus*. Allele frequencies were computed at each SNP for each group after polarizing sites using the outgroup (i.e., the ancestral allele was set to the most common allele in *D. virgineus*). Sites with missing data in any group were excluded. Statistical significance was assessed using a block-jackknife procedure with non-overlapping blocks of 500 SNPs, computing the jackknife standard error (SE) and the Z-score. Additionally, to assess whether introgression signals varied across AEOL populations, we repeated the D-statistics analysis by permuting individual AEOL populations using the approach described above.

2.5 | Demographic Scenarios

To infer the demographic history and divergence times between the two ecotypes, we performed demographic inference using ∂a∂i v2.3.0 (Gutenkunst et al. 2009). Based on the phylogenetic structure (see Figure 1C), we defined three groups and constructed a folded 3D site frequency spectrum (SFS) from the 21,935 SNPs. Using this approach, we evaluated 12 demographic models representing different evolutionary scenarios (Figure S1): (1–4) sequential divergence models (RUPI (A) → AEOL (B) → AEOL (A)), varying in presence/absence of ancestral gene flow and population bottlenecks during divergence; (5–8) alternative sequential models (RUPI (A) → AEOL (A) → AEOL (B)), varying in presence/absence of ancestral gene flow and population bottlenecks during divergence as the previous models; (9–12) scenarios assuming AEOL populations as ancestral, with RUPI derived from one of the two subclade of AEOL with or without gene flow. For the RUPI ecotype, all the demographic models included only the sister clade of AEOL. In each model, we estimated effective population sizes (N_e), divergence times (T), and migration rates (m, where applicable), which represent the proportion of each population replaced by migrants per generation. Parameters were optimized using the log-transformed optimization procedure (optimize_log) with 50 independent runs from perturbed starting values to avoid local *optima*. Each optimization run performed a maximum of 30 iterations using the BFGS algorithm. Model selection was performed using Akaike Information Criterion ($AIC = 2k - 2\ln(L)$, where k is the number of parameters and L is the maximum likelihood). Divergence times were converted to years assuming an effective ancestral population size (Na) of 10,000 individuals, a generation time of 3 years, and a mutation rate of $\mu = 7 \times 10^{-9}$ following previous studies focusing on the closely related species *D. sylvestris* and on *Silene latifolia* (Krasovec et al. 2018; Luqman et al. 2023). To assess parameter uncertainty, we performed parametric bootstrapping on the best-supported model by simulating 100 bootstrap SFS replicates under the maximum likelihood parameters with multinomial sampling variance. For each bootstrap replicate, we re-optimized all model parameters using the same optimization procedure as the original analysis.

2.6 | Estimation of Reproductive Isolation Through Reciprocal Crosses

To investigate the presence of reproductive barriers, we performed intra- and inter-ecotype reciprocal experimental crosses for a total of 314 hand pollinations in flowering seasons 2022 and 2023 using common garden plants. Flowers from at least five plants per population were bagged and

pollinated either with pollen of individuals from the same ecotype (either populations of the same or a different population of the same ecotype) or with pollen of individuals from a different ecotype. To check for the formation of fruits and seeds, approximately 20 days after pollination (DAP), we collected developed fruits on 214 crosses. Then, we counted the number of seeds per fruit as a measure of postmating prezygotic reproductive isolation and estimated seed area on all the produced seeds from the 214 crosses to assess parent-of-origin differences in seed size. Seed area was estimated from pictures with a millimetre scale as a reference using the software package Image J. All measurements were above 0.4 mm^2 and seeds displayed an elongated shape; we thus considered them undeveloped seeds rather than potential unfertilized ovules (typically rounded and smaller than 0.05 mm^2). Seeds were used to perform germination experiments. In detail, seeds were incubated without disinfection procedure at room temperature (20/10°C) and light intensity of ca. 3000 lx, in 5-cm diameter Petri dishes, on three layers of filter paper moistened with 4 mL of distilled water. Germination, that is, the emergence of a root > 2 mm, was checked at two-day intervals for the whole duration of the experiment (30 days). Germination success was recorded as a binary trait (0 = failed to germinate; 1 = seed germinated). Then, to compare trajectories of seed development, fruits in early development from a total of 100 intra- and inter-ecotype crosses were collected 3, 6, and 9 days after pollination and put in Lillie's neutral buffered formalin (Lillie 1965) until their use for optical observations. Samples were dehydrated in a graded ethanol series and embedded in Leica Historesin (Heraeus Kulzer, Hanau, Germany). Cross sections of the middle region of the ovary (5 μm thick) were sectioned on a semi-automatic rotary microtome (Leica). Serial sections were stained with toluidine blue O in phosphate–citrate buffer pH 4.5 (Sakai 1973) and mounted in Entellan synthetic resin (Merck Millipore, Burlington, MA, USA). Photomicrographs were taken with an Olympus BX 51 photomicroscope equipped with an Olympus DP71 camera.

2.7 | Statistical Analyses

2.7.1 | Phenotypic Differentiation

To investigate a putative phenotypic variation among the investigated populations, we first performed a Principal Component Analysis (PCA) using the *FactoMineR* R package (Lê et al. 2008). Trait values were centered and scaled to unit variance (*Z*-score standardization) prior to analysis to account for differences in measurement scales across traits. Then, to assess the discriminatory power of phenotypic traits in separating the two ecotypes, we performed a Linear Discriminant Analysis (LDA) using the MASS R package (Venables and Ripley 2013). To reduce dimensionality and avoid multicollinearity among correlated traits, LDA was conducted on the minimum number of PCs explaining ≥ 80% of the cumulative variance in the PCA. The discriminant function (LD1) was extracted, and classification accuracy was assessed by calculating the proportion of correctly classified individuals. Model performance was evaluated using a confusion matrix comparing predicted versus observed ecotype assignments.

2.7.2 | Estimates of Reproductive Isolation

To assess putative differences in seed number per fruit, parent-of-origin differences in seed size and germination performance among cross types (AEOL × AEOL, RUPI × RUPI, AEOL × RUPI, RUPI × AEOL), we used linear mixed models (LMMs) and generalized models (GLMMs) in the R package *lme4* (Bates et al. 2015). Cross type was treated as a fixed effect, while population was treated as a random effect. Significance of the fixed effects was tested through the Type-III Wald χ^2 tests in the R package *car* (Fox and Weisberg 2019). The *emmeans* R package (Lenth et al. 2021) was used to perform *post hoc* tests on marginal means. Following Sobel and Chen (2014), we calculated reproductive isolation (RI) index for the postmating prezygotic barrier (seed number) using the following formula:

$$RI_{PPZ} = 1 - 2 \times \left(\frac{\text{Number of seeds produced in intra} - \text{ecotype crosses}}{\text{Number of seeds produced in intra} - \text{ecotype crosses} + \text{Number of seeds produced in inter} - \text{ecotype crosses}} \right)$$

Similarly, we calculated RI index for hybrid seed inviability as follows:

$$RI_{HSI} = 1 - 2 \times \left(\frac{\text{Proportion of seeds germinated in intra} - \text{ecotype crosses}}{\text{Proportion of seeds germinated in intra} - \text{ecotype crosses} + \text{Proportion of seeds germinated in inter} - \text{ecotype crosses}} \right)$$

2.7.3 | Correlation Between Population Genetic Structure, Geography and Reproductive Isolation

To investigate the effect of geographic distance on the genetic differentiation between and within ecotypes, we performed Mantel tests using the *vegan* package (Oksanen et al. 2016). The TMA population, which included individuals from both ecotypes, was treated as two separate populations for these analyses to avoid conflating within-population and between-ecotype variation. For each pair of populations, we calculated: (i) genetic distance along PC1 and PC2 as the Euclidean distance between population-level mean PC scores and (ii) geographic distance as the great-circle distance in kilometres calculated from latitude and longitude coordinates using the *geosphere* R package (Hijmans et al. 2017). We tested correlations between these distance matrices using Mantel tests with Pearson's correlation coefficient and 9999 permutations.

3 | Results

3.1 | Ecotype Differentiation

Principal component analysis (PCA) of phenotypic traits revealed strong differentiation between the two ecotypes (Figure S2A). The first two principal components accounted for 77% of the total phenotypic variance (PC1: 55%; PC2:

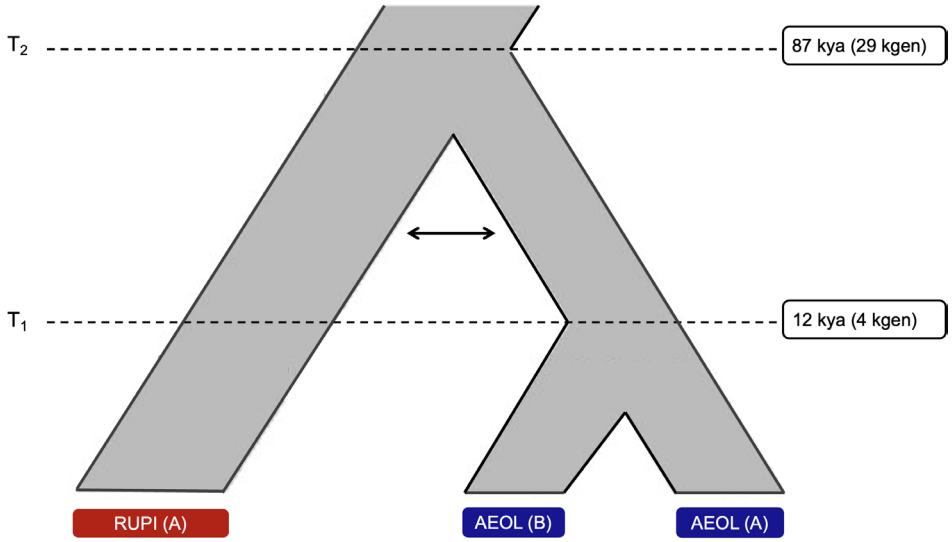

FIGURE 2 | Best-fit demographic model for two ecotypes of *Dianthus rupicola*. The best-fit demographic model estimates a split between the *rupicola* (RUPI) and *aeolicus* (AEOL) ecotype around 87 kya (95% confidence interval: 65–106 kya) and a second split between the two subclades of AEOL around 12 kya (95% confidence interval: 7–19 kya). Time is shown both in units of generation time (thousands of generations, kgen) and absolute time (thousands of years, kya), with the latter assuming a generation time of 3 years. Arrow represents bidirectional migration. Only the RUPI clade sister to AEOL that is, RUPI (A), is shown, as additional RUPI clades were not included in the demographic analyses.

22%) and clearly separated individuals into two distinct clusters corresponding to the AEOL and RUPI ecotypes, with minimal overlap between their 95% confidence ellipses. Consistently, linear discriminant analysis (LDA) performed on the first three PCs showed a very high classification accuracy (98.85%), with the discriminant function (LD1) fully separating the two ecotypes and a little overlap in their density distributions (Figure S2B). Together, these results indicate pronounced phenotypic divergence between AEOL and RUPI, with AEOL showing overall bigger flowers and a higher number of flowers per inflorescence. Patterns of phenotypic differentiation were mirrored by genomic variation. The genomic PCA (Figure 1B) showed that the first two PCs explained 27.93% of the total genomic variance (PC1: 17.04%; PC2: 10.89%) and clearly separated individuals into two distinct clusters along PC1, corresponding to the two ecotypes. In contrast, PC2 captured varying degrees of genetic differentiation among populations within each ecotype. Notably, one coastal population from northern Sicily (TMA) included individuals assigned to both AEOL and RUPI, indicating local co-occurrence of the two ecotypes. The NJ phylogenetic tree was concordant with the PCA results, revealing strong support for the separation between the RUPI and AEOL ecotypes (bootstrap support = 100%) (Figure 1C). Within the AEOL clade, populations from the Aeolian Islands (STR, SAL, LIP), two coastal populations (MIL and PAL), and few individuals from TMA formed a well-supported subclade, whereas mainland populations (TIN, MON) clustered together and showed a monophyletic origin.

3.2 | Demographic Inference

Demographic modelling highly supported a scenario of sequential divergence from the RUPI ecotype with ancestral gene flow ($m = 0.395$) and without bottleneck events (AIC = 391; Figure 2 and Table S2). The model suggests that the subclade of the AEOL ecotype including Aeolian island populations and the coastal populations MIL and PAL diverged from RUPI approximately 87 kya (95% CI: 65–106 kya). Then, more recently, approximately 12 kya (95% CI: 7–19 kya), AEOL likely colonized coastal sites of northern Sicily.

3.3 | Estimation of Reproductive Isolation Through Reciprocal Crosses

Reciprocal experimental crosses performed between the two ecotypes revealed no differences in seed number per fruit among cross types ($\chi^2 = 6.578$, $p = 0.086$), while a significant effect was observed for seed size ($\chi^2 = 174.840$, $p < 0.001$). In particular, we observed a significant reduction in seed size in inter-ecotype crosses compared to intra-ecotype crosses (Figure 3A). This reduction was also significantly different depending on which ecotype was the pollen donor ($p < 0.001$; Figure 3A). Specifically, a larger seed size was observed when AEOL populations were used as pollen donors, while smaller seeds were observed when RUPI was the pollen donor. Germination experiments showed a strong isolating barrier between the ecotypes with no seed obtained from inter-ecotype crosses being able to germinate, regardless of the cross direction ($\chi^2 = 747.00$, $p < 0.001$; Figure 3B). In line with these results, seed development observations performed at different time intervals allowed us to detect the presence of an early postzygotic barrier leading to seed inviability in inter-ecotype crosses (Figures 4 and S3). Both intra- and inter-ecotype crosses show the formation of a zygote and a free nuclear endosperm three DAP (Figure 4). Six DAP, embryos of intra-ecotype seeds were at the heart or globular stage, while in inter-ecotype seeds, embryo development was delayed or arrested at the globular stage (Figure 4). Nine DAP, in intra-ecotype seeds, embryos

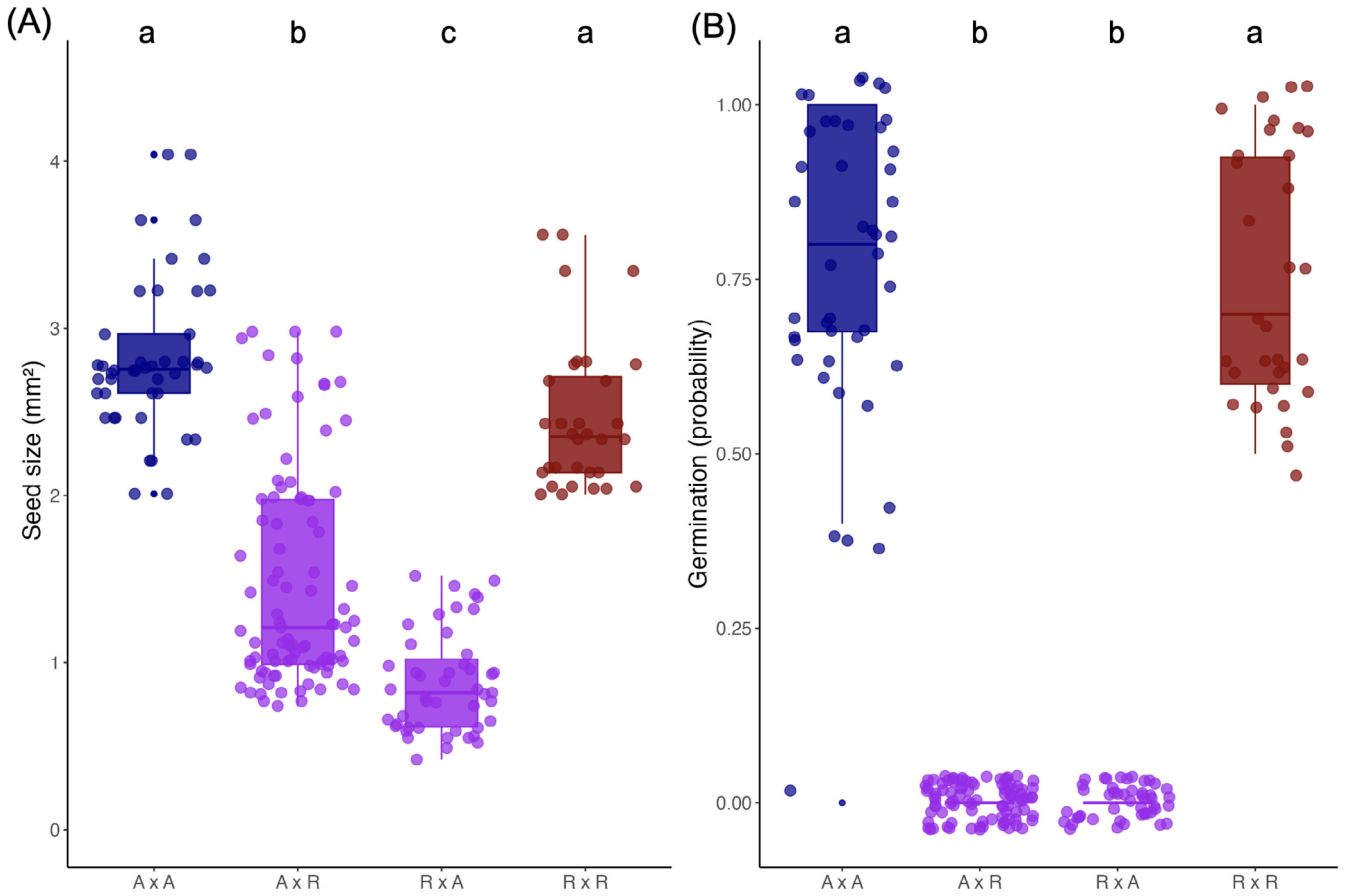

FIGURE 3 | Intra- and inter-ecotype reciprocal crosses in *Dianthus rupicola*. Differences in seed size (A) and germination performance (B) in intra-ecotype crosses within *aeolicus* (AEOL; A × A) and *rupicola* (RUPI; *R* × R) and reciprocal inter-ecotype crosses (A × *R* and *R* × A). Cross combinations are presented as pollen donor × seed parent. Different letters denote significant differences ($p < 0.05$).

were at the cotyledonary stage and endosperm appeared densely packed, while in inter-ecotype seeds, we observed a complete embryo degeneration or a delayed embryo development with particularly small embryos together with an irregularly developed endosperm (Figure 4). RI indices confirmed a negligible postmating prezygotic barrier ($RI_{PPZ} = 0.01$; 0 for AEOL and 0.02 for RUPI), whereas hybrid seed inviability was complete in both cross directions ($RI_{HSI} = 1$).

3.4 | Admixture Analyses and Hybrid Detection

The sNMF analysis identified $K = 10$ as the optimal number of genetic clusters based on the minimum cross-entropy criterion (Figures S4 and S5), reflecting the highly fragmented and isolated nature of the sampled populations. This fine-scale structure is consistent with limited gene flow among geographically isolated populations across the species' range. To visualize the broader genomic composition corresponding to the two ecotypes, we examined ancestry coefficients at $K = 2$ (Figures 5A and S5). At this hierarchical level, the individual assignment aligns with the results observed in the phenotypic analyses, the genomic PCA, and NJ tree (see Figures 1 and S2). Also, most individuals showed predominant ancestry (> 80%) to one of the two gene pools corresponding to AEOL and RUPI ecotypes, though some individuals displayed intermediate ancestry ($0.20 \leq Q \leq 0.40$). However, *Snapclust* analysis detected no recent hybrids. All individuals were assigned exclusively to pure parental clusters with high membership probabilities ($p > 0.99$; Figure 5B). The introgression analysis yielded a significantly positive *D*-statistic ($D = 0.066$, SE = 0.012, $Z = 5.41$, $p < 0.001$), indicating excess allele sharing between AEOL (B) and RUPI (A) beyond what is expected under incomplete lineage sorting alone. Permutation of individual AEOL populations revealed that the introgression signal was consistent across AEOL (B) populations.

3.5 | Correlation Between Population Genetic Structure and Geography

To link patterns of genomic differentiation with geographic structure, we tested for a correlation between genetic and geographic distance. The first genomic PC1 was not significantly correlated with geographic distance (Mantel $r = 0.126$, $p = 0.081$), while PC2 showed a significant correlation with geographic distance (Mantel $r = 0.275$, $p = 0.015$). This result indicates that PC2 captures genetic structure arising from spatial isolation and limited gene flow among fragmented populations within each ecotype.

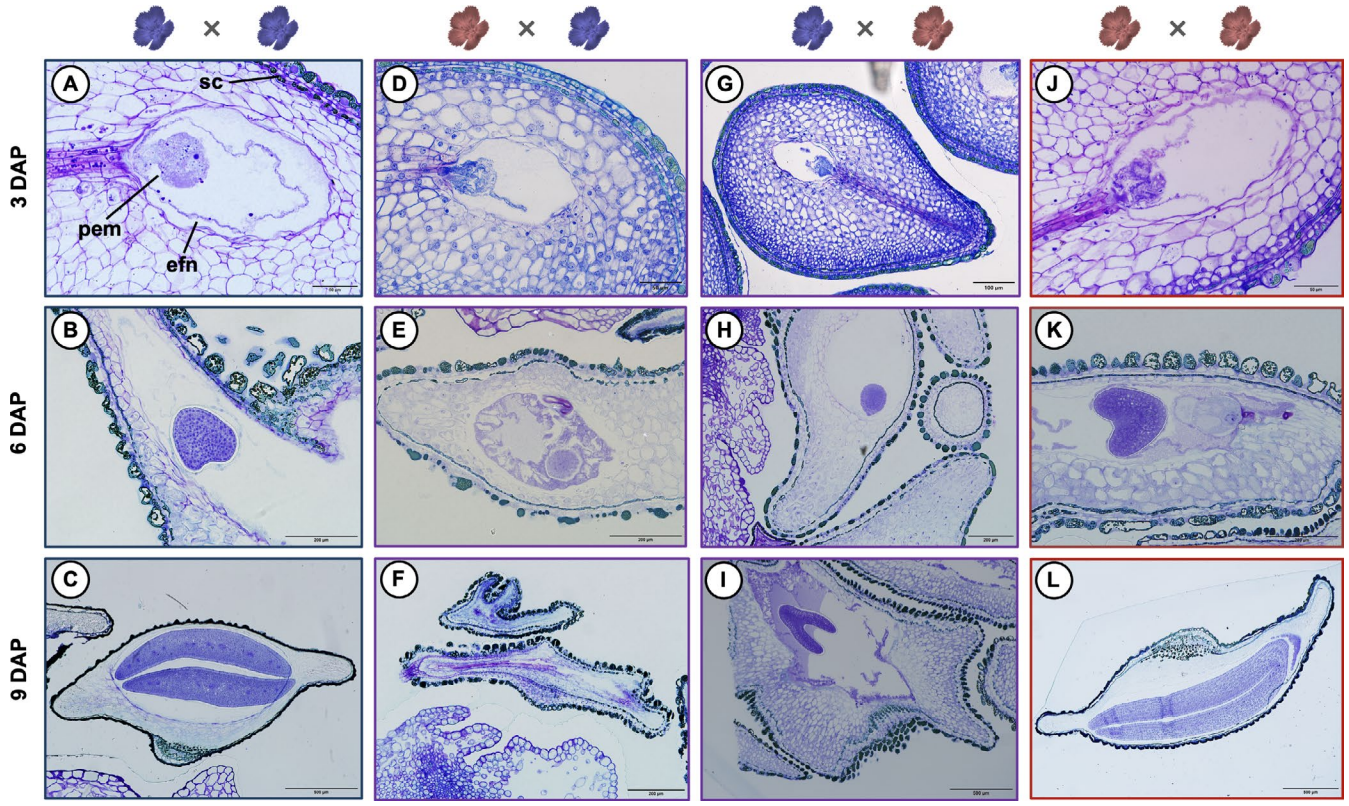

FIGURE 4 | Intra- and inter-ecotype reciprocal crosses in *Dianthus rupicola*. Seed development was observed at 3 (A, D, G, J), 6 (B, E, H, K) and 9 days after pollination (DAP; C, F, I, L). Red denotes the *rupicola* ecotype (RUPI) and blue denotes the *aeolicus* ecotype (AEOL). Cross combinations are presented as pollen donor × seed parent. pem, proembryo; efn, endosperm free nucleus; sc, seed coat. The panels display the most advanced developmental stage observed for each cross type at the indicated time points. The broader developmental variation within these crosses is detailed in Figure S3.

4 | Discussion

Investigating the early phases of divergence between closely related lineages contributes to understanding the processes that trigger plant diversification and is especially important in groups experiencing unusually fast evolutionary radiations (Via 2009; Pinheiro et al. 2018). Here, we investigated the early divergence of two ecotypes of the rapidly evolving *D. rupicola* group, a species complex belonging to the Eurasiatic clade of the genus *Dianthus*, that is, the clade experiencing the fastest radiation among flowering plants (Valente et al. 2010).

Our phenotypic analyses of 11 populations of *D. rupicola* clearly identify the presence of two clusters, one occurring primarily on the Aeolian archipelago and in a few ecologically connected coastal populations (identified as AEOL) and the other with a broader distribution in Sicily and in southern peninsular Italy (identified as RUPI). This pattern was strongly supported by our genomic analyses. Indeed, population assignments were consistently confirmed by PCA, phylogenetic reconstruction, and admixture analyses, although, as expected, the latter analysis identified optimal values of *K* approaching the number of sampled populations due to strong population fragmentation and fine-scale genetic structure within ecotypes.

Phylogenetic reconstruction including a closely related taxon belonging to the *D. virgineus* group further confirmed that AEOL and RUPI are sister lineages (as also shown in Fassou et al. 2022), with AEOL forming a monophyletic group nested within RUPI. Within AEOL, populations were subdivided into two well-supported subclades, one comprising the Aeolian island populations together with the coastal populations MIL and PAL, and the other including Sicilian populations (MON and TIN). This hierarchical structure highlights a complex history of divergence and complicates inference about the precise geographic origin, timing, and levels of gene flow during early differentiation. To resolve these questions, we tested multiple alternative demographic scenarios informed by phylogenetic relationships. Our analyses support a scenario in which the AEOL ecotype originated from RUPI approximately 87 kya, indicating that divergence between the two ecotypes represents a very recent event within the Eurasiatic *Dianthus* clade, which began diversifying around 2.5 MYA (Valente et al. 2010). The AEOL group including the Aeolian island populations and the coastal populations PAL and MIL appears to have diverged first, followed by a more recent split involving Sicilian coastal populations (MON and TIN) around 12 kya. This pattern is consistent with a scenario in which geographic fragmentation, typical of this *Dianthus* complex, triggered initial divergence from the more widespread RUPI ecotype, with subsequent secondary colonization of Sicily. Our results thus suggest that the intra-ecotype divergence of the AEOL ecotype likely reflects a recent return, after a period of isolation likely on the Aeolian archipelago, to the Sicilian island.

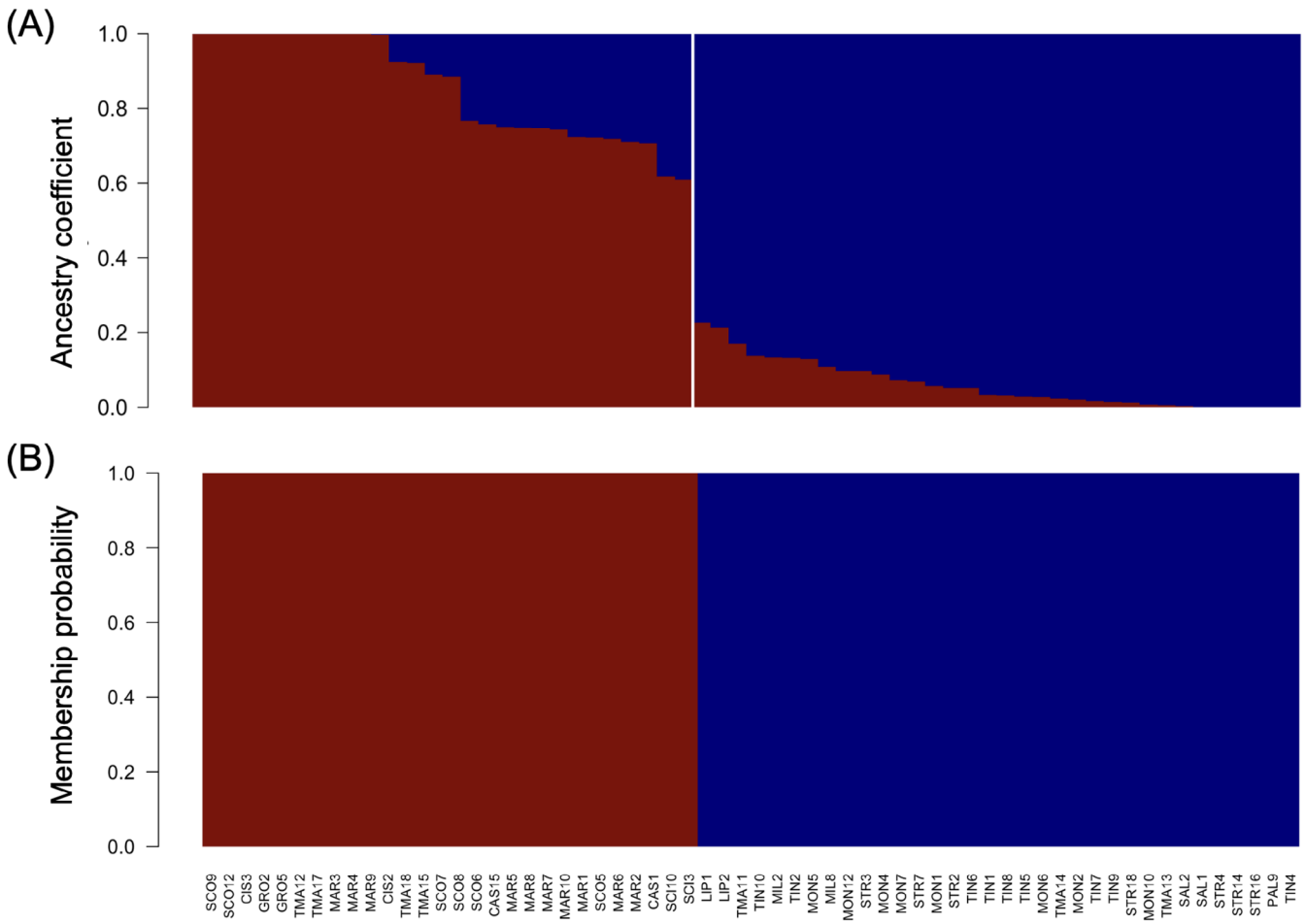

FIGURE 5 | Admixture analyses and hybrid detection in two *Dianthus rupicola* ecotypes. Ancestry coefficients of *Dianthus rupicola* populations estimated for $K = 2$ (A); genotype composition obtained in the search for hybrids using hybridization coefficient for $F_1 = 0.5$ and first backcross = 0.25 (B). Blue denotes the *aeolicus* ecotype (AEOL), while red denotes the *rupicola* ecotype (RUPI).

Overall, the very recent timing of divergence, combined with the close phylogenetic relationship and partial geographic overlap between the two ecotypes, makes our study system a suitable model to investigate the ecological and intrinsic processes characterizing the earliest phases of divergence in a complex of the *Dianthus* genus.

Divergence between geographical segregates, as we found in our study system, is a common output of populations with restricted gene flow. However, plant diversification also requires the incipient arising of some form of reproductive isolation between diverging lineages (Lowry and Gould 2016; Christie et al. 2022; Butlin and Faria 2024). In our study system, since premating barriers are extremely weak, we investigated postmating barriers by performing reciprocal crosses between the two ecotypes. By doing this, we found no evidence of a reduced number of seeds in inter-ecotype relative to intra-ecotype crosses, indicating a lack of postmating prezygotic barriers ($RI_{PPZ} = 0.01$; 0 in AEOL and 0.02 in RUPI). Instead, we observed that none of the seeds produced in inter-ecotype crosses germinated, revealing a strong hybrid seed inviability barrier ($RI_{HSI} = 1$ in both directions).

Our experimental design also allowed us to observe developing seeds at different time intervals (3, 6, 9 days after pollination) and thus to elucidate the mechanisms underlying hybrid seed inviability in inter-ecotype crosses, as well as the developmental stage at which it occurs. Fertilization occurred successfully in both intra- and inter-ecotype crosses, as evidenced by zygote formation and early endosperm development at 3 days after pollination. However, by 6 days after pollination, embryo development in inter-ecotype seeds was delayed or arrested at the globular stage, whereas intra-ecotype embryos progressed normally. By 9 days after pollination, intra-ecotype seeds contained cotyledonary-stage embryos and a well-developed endosperm, while inter-ecotype seeds were largely degenerated or, in rare cases, exhibited severely reduced embryos accompanied by irregular endosperm proliferation. These observations, coupled with the weakness of premating and postmating prezygotic barriers, identify hybrid seed inviability as the first strong reproductive barrier separating AEOL and RUPI and implicate disrupted endosperm development as its mechanistic basis.

A similar endosperm-linked barrier associated with hybrid seed viability is emerging as a common mechanism of reproductive isolation in many angiosperm groups (Dowrick and Brandram 1970; Pal and Khoshoo 1972; Johnston and Hanneman Jr 1982; Lester and Kang 1998; Scott et al. 1998; Fu et al. 2009), including fast radiating ones (Briscoe Runquist

et al. 2014; Oneal et al. 2016; İltaş et al. 2021). This barrier, by acting in the F_1 generation, may represent a formidable reproductive barrier and may lead, as in our case, to nearly complete reproductive isolation also on a short timescale (Coughlan 2023). In our study system, the absence of other barriers and the strong hybrid seed inviability observed in both cross directions suggest that this developmental incompatibility represents the first mechanism responsible for a reduction of gene flow in these recently diverged lineages and is thus directly involved in speciation. Comparable results were reported in closely related species of the genus *Mimulus*, where hybrid seed inviability emerged as the primary reproductive barrier (e.g., Oneal et al. 2016; Sandstedt and Sweigart 2022). In *Dianthus*, this barrier has never been explicitly reported to play a role in diversification. However, classical studies describe the presence of degenerating embryos in experimental crosses conducted between different *Dianthus* species suggesting that it can be a common mechanism within the genus (Buell 1953; Carolin 1957; Nimura et al. 2003).

Our findings generate a variety of hypotheses about the mechanisms that are controlling the emergence of this barrier. Under the EBN framework, the main mechanism invoked as a promoter of hybrid seed inviability is a disruption of the 2:1 maternal-to-paternal genomic ratio required for proper endosperm formation, which leads to dysfunctional endosperm development and, ultimately, aborted seeds (Köhler et al. 2003; Reyes and Grossniklaus 2003; Josefsson et al. 2006; Kradolfer et al. 2013). Such dosage imbalances could underlie failures also in homoploid crosses, as reported in several study systems (e.g., Oneal et al. 2016; Lafon-Placette et al. 2017, 2018; Coughlan et al. 2020; Sandstedt and Sweigart 2022), via changes in imprinting status, sequence divergence or gene duplication, all of which might alter the balance of dosage-sensitive genes necessary for normal seed development (Johnston and Hanneman Jr 1982; Birchler and Veitia 2010; Köhler et al. 2010, 2012; Birchler 2014; Wolff et al. 2015; Garner et al. 2016). In line with the EBN theory, in our study, we also observed a strong asymmetric difference in seed size between reciprocal crosses, yet neither cross direction produced germinable seeds and both hybrid seed phenotypes were smaller than those of either parental ecotype. Specifically, when AEOL acts as a pollen donor, seeds were significantly larger than in the reciprocal cross, thus suggesting that AEOL may drive excessive endosperm growth producing larger but inviable seeds, a hallmark of paternal excess (Coughlan 2023). These findings are consistent with the well-known parent-of-origin asymmetry in seed phenotypes resulting from an EBN divergence between crossed taxa (Lafon-Placette et al. 2018; Coughlan et al. 2020; İltaş et al. 2021; Sandstedt and Sweigart 2022). Also, our observations align with previous studies showing that systems with strong symmetric hybrid seed inviability, although exhibiting parent-of-origin effects on seed size, show smaller seeds in both cross directions compared to parental species (Lafon-Placette et al. 2017; Roth et al. 2018; Coughlan et al. 2020). These patterns are possibly linked to stronger endosperm defects which arise earlier in development and thus trigger premature seed abortion (Coughlan et al. 2020). The drivers of EBN divergence in homoploid taxa have been associated either to life-history traits (e.g., breeding system), demographic or ecological factors (see e.g., Briscoe Runquist et al. 2014; Coughlan et al. 2020; Florez-Rueda et al. 2021; Frayer et al. 2026). In our study system, the two ecotypes show the same breeding system, suggesting that EBN differences did not arise as a consequence of mating system shifts. It is, instead, plausible, as reported in Coughlan et al. (2020), that geographic isolation and demographic history may have promoted the fixation of alleles affecting dosage-sensitive imprinted genes. Notably, the two ecotypes also differ in several ecological and genomic factors, that is, antagonistic interactions, edaphic conditions and genome size, opening the possibility that these differences may have contributed to EBN divergence.

Beyond the implications on the initial phase of divergence, our study also allows us to test the admixture between these recently diverged ecotypes. This goal is important in our study system but also contributes to gaining insights into the survival potential of the multitude of endemic and geographically isolated *Dianthus* taxa in secondary contact, which is predicted to become common under a climate change scenario (e.g., Gómez et al. 2015). Our genomic analyses revealed low but detectable signals of admixture between the two ecotypes. However, a clear differentiation was observed in the TMA population, where AEOL and RUPI individuals occur in sympatry. Also, the discrete classification analysis rejected the hypothesis of recent hybridization, as no individuals were assigned to F_1 or early backcross categories despite the admixture coefficients observed in sNMF. The absence of detectable hybrids suggests that these signals most likely reflect ancestral polymorphism or rare hybridization events followed by limited backcrossing, rather than ongoing gene flow. In line with the latter hypothesis, we observed excess allele sharing between Sicilian populations of AEOL and RUPI, consistent with a scenario of past introgression in Sicily. Clearly, we employed a limited number of individuals overall, and thus we cannot rule out the possibility of an underestimation of the admixture in our analyses. Nevertheless, the concordance between genomic differentiation and experimental crossing results suggests that hybrid seed inviability is highly effective in maintaining reproductive isolation allowing the survival of the two ecotypes upon secondary contact.

5 | Conclusions

Our study shed light on the early phase of divergence between two closely related ecotypes of *Dianthus*, supporting a scenario in which divergence was triggered by geographic fragmentation. Genomic analyses indicate a clear genetic separation between ecotypes with low admixture, while reciprocal crossing experiments demonstrate that postzygotic isolation, mediated by hybrid seed inviability, rapidly evolved. The asymmetric pattern of seed size between reciprocal crosses suggests a divergence in EBN between the two ecotypes and places *D. rupicola* within the growing body of evidence that parent-of-origin effects on endosperm development represent a common and rapidly evolving mechanism of reproductive isolation in angiosperms. Future work disentangling the relative contributions of ecological differentiation and island colonization to EBN divergence and identifying the imprinted genes disrupted in inter-ecotype crosses will be essential to elucidate the ultimate drivers of the rapid evolution of hybrid seed inviability in the fastest documented radiation of flowering plants.

Author Contributions

Lucrezia Laccetti: conceptualization, investigation, data curation, formal analysis, visualization, methodology, writing – original draft, writing – review and editing. **Donata Cafasso:** data curation, formal analysis, writing – review and editing. **Teresa R. Galise:** data curation, formal analysis, writing – review and editing. **Antonia Cristaudo:** investigation, data curation, writing – review and editing. **Bárbara S. Santos Leal:** data curation, methodology, writing – review and editing. **João Pedro S. Pena Bento:** investigation, formal analysis, visualization, methodology, writing – review and editing. **Juliana L. Sampaio Mayer:** investigation, data curation, visualization, writing – review and editing. **Fabio Pinheiro:** data curation, formal analysis, writing – review and editing. **Giovanni Scopece:** conceptualization, investigation, methodology, project administration, writing – original draft, writing – review and editing. All authors gave final approval for submission and agreed to be held accountable for the work performed therein.

Acknowledgements

The authors thank Fabiana De Vita, William Coppola, and Andrea Capuano for their help in experimental procedures. They also thank Luca D'Aniello, Mariella Masucci, Pino Marrucci, and Valentina Tranchida Lombardo for their help and support during fieldwork and the Italian Ministero dell'Ambiente e della Sicurezza Energetica for issuing the collecting licence (PNM_03-18935-2023-0088).

Funding

G.S. and L.L. were funded in the frame of the PRIN2022PNRR-URBANPOLL funded by the European Union—NextGenerationEU, Mission 4 Component 1 CUP E53D23014450001. L.L. was also funded in the frame of the Ph.D. scholarship in the field of sustainable development financially supported by INPS (National Institute of Social Insurance). D.C. was funded under the Project FRA-HYSENSING CUP E65F22000050001, financially supported by the University of Naples Federico II.

Ethics Statement

The authors have nothing to report.

Conflicts of Interest

The authors declare no conflicts of interest.

Data Availability Statement

All the data supporting the findings of this study are openly available in the Figshare repository (https://doi.org/10.6084/m9.figshare.32301912).

References

Balao, F., L. M. Valente, P. Vargas, J. Herrera, and S. Talavera. 2010. "Radiative Evolution of Polyploid Races of the Iberian Carnation *Dianthus broteri* (Caryophyllaceae)." *New Phytologist* 187: 542–551.

Bates, D., M. Mächler, B. Bolker, and S. Walker. 2015. "Fitting Linear Mixed-Effects Models Using lme4." *Journal of Statistical Software* 67: 1–48.

Bedinger, P. A., R. T. Chetelat, B. McClure, et al. 2011. "Interspecific Reproductive Barriers in the Tomato Clade: Opportunities to Decipher Mechanisms of Reproductive Isolation." *Sexual Plant Reproduction* 24: 171–187.

Beugin, M. P., T. Gayet, D. Pontier, S. Devillard, and T. Jombart. 2018. "A Fast Likelihood Solution to the Genetic Clustering Problem." *Methods in Ecology and Evolution* 9: 1006–1016.

Birchler, J. A. 2014. "Interploidy Hybridization Barrier of Endosperm as a Dosage Interaction." *Frontiers in Plant Science* 5: 281.

Birchler, J. A., and R. A. Veitia. 2010. "The Gene Balance Hypothesis: Implications for Gene Regulation, Quantitative Traits and Evolution." *New Phytologist* 186: 54–62.

Bittrich, V. 1993. "Caryophyllaceae." In *The Families and Genera of Vascular Plants II Flowering Plants—Dicotyledons Magnoliid, Hamamelid and Caryophyllid Families*, edited by K. Kubitzki, G. Rohwer, and V. Bittrich, 206–236. Springer-Verlag.

Briscoe Runquist, R. D., E. Chu, J. L. Iverson, J. C. Kopp, and D. A. Moeller. 2014. "Rapid Evolution of Reproductive Isolation Between Incipient Outcrossing and Selfing *Clarkia* Species." *Evolution* 68: 2885–2900.

Brullo, S., and P. Minissale. 2001. "Il Gruppo di *Dianthus rupicola* Biv. Nel Mediterraneo Centrale." *Informatore Botanico Italiano* 33: 537–542.

Buell, K. M. 1953. "Developmental Morphology in *Dianthus*. III. Seed Failure Following Interspecific Crosses." *American Journal of Botany* 40: 116–123.

Bushell, C., M. Spielman, and R. J. Scott. 2003. "The Basis of Natural and Artificial Postzygotic Hybridization Barriers in *Arabidopsis* Species." *Plant Cell* 15: 1430–1442.

Butel, N., Y. Qiu, W. Xu, J. Santos-González, and C. Köhler. 2024. "Parental Conflict Driven Regulation of Endosperm Cellularization by a Family of Auxin Response Factors." *Nature Plants* 10: 1018–1026.

Butlin, R. K., and R. Faria. 2024. "Local Adaptation and Reproductive Isolation: When Does Speciation Start?" *Evolutionary Journal of the Linnean Society* 3: kzae003.

Cahenzli, F., C. Bonetti, and A. Erhardt. 2018. "Divergent Strategies in Pre- and Postzygotic Reproductive Isolation Between Two Closely Related *Dianthus* Species." *Evolution* 72: 1851–1862.

Carolin, R. C. 1957. "Cytological and Hybridization Studies in the Genus *Dianthus*." *New Phytologist* 56: 81–97.

Christie, K., L. S. Fraser, and D. B. Lowry. 2022. "The Strength of Reproductive Isolating Barriers in Seed Plants: Insights From Studies Quantifying Premating and Postmating Reproductive Barriers Over the Past 15 Years." *Evolution* 76: 2228–2243.

Coughlan, J. M. 2023. "The Role of Conflict in Shaping Plant Biodiversity." *New Phytologist* 240: 2210–2217.

Coughlan, J. M., M. W. Brown, and J. H. Willis. 2020. "Patterns of Hybrid Seed Inviability in the *Mimulus guttatus* sp. Complex Reveal a Potential Role of Parental Conflict in Reproductive Isolation." *Current Biology* 30: 83–93.

Domina, G., S. Scibetta, F. Scafidi, and A. Giovino. 2017. "Contribution to the Identification of *Dianthus rupicola* (Caryophyllaceae) Subspecies Using Morphological and Molecular Approaches." *Phytotaxa* 291: 17–32.

Dowrick, G. J., and S. N. Brandram. 1970. "Abnormalities of Endosperm Development in *Lilium* Hybrids." *Euphytica* 19: 433–442.

Dziasek, K., J. Santos-González, K. Wang, et al. 2024. "Dosage-Sensitive Maternal siRNAs Determine Hybridization Success in *Capsella*." *Nature Plants* 10: 1969–1983.

Fassou, G., N. Korotkova, A. Nersesyan, M. A. Koch, P. Dimopoulos, and T. Borsch. 2022. "Taxonomy of *Dianthus* (Caryophyllaceae)–Overall Phylogenetic Relationships and Assessment of Species Diversity Based on a First Comprehensive Checklist of the Genus." *Phytokeys* 196: 91–214.

Florez-Rueda, A. M., M. Scharmann, M. Roth, and T. Städler. 2021. "Population Genomics of the "Arcanum" Species Group in Wild Tomatoes: Evidence for Separate Origins of Two Self-Compatible Lineages." *Frontiers in Plant Science* 12: 624442.

Fox, J., and S. Weisberg. 2019. *An R Companion to Applied Regression*. 3rd ed. Sage.

Frayer, M. E., H. K. Soliman, P. F. Schwarz, and J. M. Coughlan. 2026. "Introgression and Parental Conflict Shape Repeated Occurrences of Postzygotic Isolation in *Mimulus*." *Current Biology* 36: 1454–1467.

Frichot, E., and O. François. 2015. "LEA: An R Package for Landscape and Ecological Association Studies." *Methods in Ecology and Evolution* 6: 925–929.

Frichot, E., F. Mathieu, T. Trouillon, G. Bouchard, and O. François. 2014. "Fast and Efficient Estimation of Individual Ancestry Coefficients." *Genetics* 196: 973–983.

Fu, X. L., Y. G. Lu, X. D. Liu, and J. Q. Li. 2009. "Crossability Barriers in the Interspecific Hybridization Between *Oryza sativa* and *O. meyeriana*." *Journal of Integrative Plant Biology* 51: 21–28.

Garner, A. G., A. M. Kenney, L. Fishman, and A. L. Sweigart. 2016. "Genetic Loci With Parent-of-Origin Effects Cause Hybrid Seed Lethality in Crosses Between *Mimulus* Species." *New Phytologist* 211: 319–331.

Givnish, T. J., D. Spalink, M. Ames, et al. 2015. "Orchid Phylogenomics and Multiple Drivers of Their Extraordinary Diversification." *Proceedings of the Royal Society B* 282: 20151553.

Gómez, J. M., A. González-Megías, J. Lorite, M. Abdelaziz, and F. Perfectti. 2015. "The Silent Extinction: Climate Change and the Potential Hybridization-Mediated Extinction of Endemic High-Mountain Plants." *Biodiversity and Conservation* 24: 1843–1857.

Green, R. E., J. Krause, A. W. Briggs, et al. 2010. "A Draft Sequence of the Neandertal Genome." *Science* 328: 710–722.

Gutenkunst, R. N., R. D. Hernandez, S. H. Williamson, and C. D. Bustamante. 2009. "Inferring the Joint Demographic History of Multiple Populations From Multidimensional SNP Frequency Data." *PLoS Genetics* 5: e1000695.

Gutierrez-Marcos, J. F., P. D. Pennington, L. M. Costa, and H. G. Dickinson. 2003. "Imprinting in the Endosperm: A Possible Role in Preventing Wide Hybridization." *Philosophical Transactions of the Royal Society B* 358: 1105–1111.

Haig, D., and M. Westoby. 1989. "Parent-Specific Gene Expression and the Triploid Endosperm." *American Naturalist* 134: 147–155.

Hijmans, R. J., E. Williams, C. Vennes, and M. R. J. Hijmans. 2017. "Package 'geosphere'." *Spherical Trigonometry* 1: 1–45.

İltaş, Ö., M. Svitok, A. Cornille, R. Schmickl, and C. Lafon Placette. 2021. "Early Evolution of Reproductive Isolation: A Case of Weak Inbreeder/Strong Outbreeder Leads to an Intraspecific Hybridization Barrier in *Arabidopsis lyrata*." *Evolution* 75: 1466–1476.

Johnston, S. A., T. P. M. Den Nijs, S. J. Peloquin, and R. E. Hanneman Jr. 1980. "The Significance of Genic Balance to Endosperm Development in Interspecific Crosses." *Theoretical and Applied Genetics* 57: 5–9.

Johnston, S. A., and R. E. Hanneman Jr. 1982. "Manipulations of Endosperm Balance Number Overcome Crossing Barriers Between Diploid *Solanum* Species." *Science* 217: 446–448.

Jombart, T. 2008. "adegenet: A R Package for the Multivariate Analysis of Genetic Markers." *Bioinformatics* 24: 1403–1405.

Josefsson, C., B. Dilkes, and L. Comai. 2006. "Parent-Dependent Loss of Gene Silencing During Interspecies Hybridization." *Current Biology* 16: 1322–1328.

Katoch, M., K. Verma, D. Sharma, et al. 2024. "Ornamental Plant Breeding for Improved Floral Attributes: Entering a New Era." In *Ornamental Horticulture: Latest Cultivation Practices and Breeding Technologies*, 45–62. Springer Nature.

Köhler, C., L. Hennig, R. Bouveret, J. Gheyselinck, U. Grossniklaus, and W. Gruissem. 2003. "Arabidopsis MSI1 Is a Component of the MEA/FIE Polycomb Group Complex and Required for Seed Development." *EMBO Journal* 22: 4804–4814.

Köhler, C., O. M. Scheid, and A. Erilova. 2010. "The Impact of the Triploid Block on the Origin and Evolution of Polyploid Plants." *Trends in Genetics* 26: 142–148.

Köhler, C., P. Wolff, and C. Spillane. 2012. "Epigenetic Mechanisms Underlying Genomic Imprinting in Plants." *Annual Review of Plant Biology* 63: 331–352.

Kong, H., F. L. Condamine, L. Yang, et al. 2022. "Phylogenomic and Macroevolutionary Evidence for an Explosive Radiation of a Plant Genus in the Miocene." *Systematic Biology* 71: 589–609.

Kradolfer, D., P. Wolff, H. Jiang, A. Siretskiy, and C. Köhler. 2013. "An Imprinted Gene Underlies Postzygotic Reproductive Isolation in *Arabidopsis thaliana*." *Developmental Cell* 26: 525–535.

Krasovec, M., M. Chester, K. Ridout, and D. A. Filatov. 2018. "The Mutation Rate and the Age of the Sex Chromosomes in *Silene latifolia*." *Current Biology* 28: 1832–1838.

Laccetti, L., E. Petrone-Mendoza, D. Cafasso, A. Cristaudo, F. Pinheiro, and G. Scopece. 2026. "Linking Genome Size Variation to Phenotypic Selection on Target Traits." *Ecology* in press.

Lafon-Placette, C., M. R. Hatorangan, K. A. Steige, et al. 2018. "Paternally Expressed Imprinted Genes Associate With Hybridization Barriers in Capsella." *Nature Plants* 4: 352–357.

Lafon-Placette, C., I. M. Johannessen, K. S. Hornslien, et al. 2017. "Endosperm-Based Hybridization Barriers Explain the Pattern of Gene Flow Between Arabidopsis Lyrata and *Arabidopsis arenosa* in Central Europe." *Proceedings of the National Academy of Sciences* 114: E1027–E1035.

Lafon-Placette, C., and C. Köhler. 2016. "Endosperm-Based Postzygotic Hybridization Barriers: Developmental Mechanisms and Evolutionary Drivers." *Molecular Ecology* 25: 2620–2629.

Lagomarsino, L. P., F. L. Condamine, A. Antonelli, A. Mulch, and C. C. Davis. 2016. "The Abiotic and Biotic Drivers of Rapid Diversification in Andean Bellflowers (Campanulaceae)." *New Phytologist* 210: 1430–1442.

Lê, S., J. Josse, and F. Husson. 2008. "FactoMineR: An R Package for Multivariate Analysis." *Journal of Statistical Software* 25: 1–18.

Leapman, M. 2012. *The Ingenious Mr Fairchild: The Forgotten Father of the Flower Garden*. Faber & Faber.

Lenth, R., H. Singmann, J. Love, P. Buerkner, and M. Herve. 2021. "Emmeans: Estimated Marginal Means, Aka Least-Squares Means (R Package Version 1.5.1.) [Computer Software]." *The Comprehensive R Archive Network*. https://CRAN.R-project.org/package=emmeans.

Lester, R. N., and J. H. Kang. 1998. "Embryo and Endosperm Function and Failure in *Solanum* Species and Hybrids." *Annals of Botany* 82: 445–453.

Lillie, R. D. 1965. *Histopathologic Technic and Practical Histochemistry*. McGraw Hill.

Lowry, D. B., and B. A. Gould. 2016. "Speciation Continuum." In *Encyclopedia of Evolutionary Biology*, edited by R. Kliman and D. Ortiz-Barrientos, 159–165. Elsevier, Online Publication.

Luqman, H., D. Wegmann, S. Fior, and A. Widmer. 2023. "Climate-Induced Range Shifts Drive Adaptive Response via Spatio-Temporal Sieving of Alleles." *Nature Communications* 14: 1080.

Malinsky, M., M. Matschiner, and H. Svardal. 2021. "Dsuite-Fast D-Statistics and Related Admixture Evidence From VCF Files." *Molecular Ecology Resources* 21: 584–595.

Martin, S. H., J. W. Davey, and C. D. Jiggins. 2015. "Evaluating the Use of ABBA–BABA Statistics to Locate Introgressed Loci." *Molecular Biology and Evolution* 32: 244–257.

Moyle, L. C., M. S. Olson, and P. Tiffin. 2004. "Patterns of Reproductive Isolation in Three Angiosperm Genera." *Evolution* 58: 1195–1208.

Nimura, M., J. Kato, M. Mii, and K. Morioka. 2003. "Unilateral Compatibility and Genotypic Difference in Crossability in Interspecific Hybridization Between *Dianthus caryophyllus* L. and *Dianthus japonicus* Thunb." *Theoretical and Applied Genetics* 106: 1164–1170.

Oksanen, J., F. G. Blanchet, R. Kindt, et al. 2016. "Vegan: Community Ecology Package." R Package Version 2.3-3. https://CRAN.R-project.org/package=vegan.

Oneal, E., J. H. Willis, and R. G. Franks. 2016. "Disruption of Endosperm Development Is a Major Cause of Hybrid Seed Inviability Between *Mimulus guttatus* and *Mimulus nudatus*." *New Phytologist* 210: 1107–1120.

Pal, M., and T. N. Khoshoo. 1972. "Evolution and Improvement of Cultivated Amaranths. IV. Variation in Pollen Mitosis in the F1 *Amaranthus spinosus* × *A. dubius*." *Genetica* 43: 119–129.

Paradis, E., and K. Schliep. 2019. "Ape 5.0: An Environment for Modern Phylogenetics and Evolutionary Analyses in R." *Bioinformatics* 35: 526–528.

Peterson, B. K., J. N. Weber, E. H. Kay, H. S. Fisher, and H. E. Hoekstra. 2012. "Double Digest RADseq: An Inexpensive Method for de Novo SNP Discovery and Genotyping in Model and Non-Model Species." *PLoS One* 7: e37135.

Pinheiro, F., M. V. Dantas-Queiroz, and C. Palma-Silva. 2018. "Plant Species Complexes as Models to Understand Speciation and Evolution: A Review of South American Studies." *Critical Reviews in Plant Sciences* 37: 54–80.

Pritchard, J. K., M. Stephens, N. A. Rosenberg, and P. Donnelly. 2000. "Association Mapping in Structured Populations." *American Journal of Human Genetics* 67: 170–181.

Queller, D. C. 1983. "Kin Selection and Conflict in Seed Maturation." *Journal of Theoretical Biology* 100: 153–172.

R Core Team. 2024. *R: A Language and Environment for Statistical Computing*. R Foundation for Statistical Computing.

Reyes, J. C., and U. Grossniklaus. 2003. "Diverse Functions of Polycomb Group Proteins During Plant Development." *Seminars in Cell & Developmental Biology* 14: 77–84.

Rochette, N. C., A. G. Rivera-Colón, and J. M. Catchen. 2019. "Stacks 2: Analytical Methods for Paired-End Sequencing Improve RADseq-Based Population Genomics." *Molecular Ecology* 28: 4737–4754.

Roth, M., A. M. Florez-Rueda, S. Griesser, M. Paris, and T. Städler. 2018. "Incidence and Developmental Timing of Endosperm Failure in Post-Zygotic Isolation Between Wild Tomato Lineages." *Annals of Botany* 121: 107–118.

Sakai, W. S. 1973. "Simple Method for Differential Staining of Paraffin Embedded Plant Material Using Toluidine Blue O." *Stain Technology* 48: 247–249.

Sandstedt, G. D., and A. L. Sweigart. 2022. "Developmental Evidence for Parental Conflict in Driving *Mimulus* Species Barriers." *New Phytologist* 236: 1545–1557.

Scopece, G., C. Lexer, A. Widmer, and S. Cozzolino. 2010. "Polymorphism of Postmating Reproductive Isolation Within Plant Species." *Taxon* 59: 1367–1374.

Scott, R. J., M. Spielman, J. Bailey, and H. G. Dickinson. 1998. "Parent-of-Origin Effects on Seed Development in *Arabidopsis thaliana*." *Development* 125: 3329–3341.

Sedeek, K. E., G. Scopece, Y. M. Staedler, et al. 2014. "Genic Rather Than Genome-Wide Differences Between Sexually Deceptive *Ophrys* Orchids With Different Pollinators." *Molecular Ecology* 23: 6192–6205.

Sobel, J. M. 2014. "Ecogeographic Isolation and Speciation in the Genus *Mimulus*." *American Naturalist* 184: 565–579.

Sobel, J. M., and G. F. Chen. 2014. "Unification of Methods for Estimating the Strength of Reproductive Isolation." *Evolution* 68: 1511–1522.

Suni, S. S., and R. Hopkins. 2018. "The Relationship Between Postmating Reproductive Isolation and Reinforcement in *Phlox*." *Evolution* 72: 1387–1398.

Valente, L. M., V. Savolainen, and P. Vargas. 2010. "Unparalleled Rates of Species Diversification in Europe." *Proceedings of the Royal Society B* 277: 1489–1496.

Venables, W. N., and B. D. Ripley. 2013. *Modern Applied Statistics With S*. Springer Science & Business Media.

Via, S. 2009. "Natural Selection in Action During Speciation." *Proceedings of the National Academy of Sciences of the United States of America* 106: 9939–9946.

Weng, Y., H. Li, J. Yang, and Z. Q. Zhang. 2023. "The Past, Present, and Future of Ecogeographic Isolation Between Closely Related Aquilegia Plants." *Ecology and Evolution* 13: e10098.

Wolff, P., H. Jiang, G. Wang, J. Santos-González, and C. Köhler. 2015. "Paternally Expressed Imprinted Genes Establish Postzygotic Hybridization Barriers in *Arabidopsis thaliana*." *eLife* 4: e10074.

Yu, G., D. K. Smith, H. Zhu, Y. Guan, and T. T. Y. Lam. 2017. "ggtree: An R Package for Visualization and Annotation of Phylogenetic Trees With Their Covariates and Other Associated Data." *Methods in Ecology and Evolution* 8: 28–36.

Zeh, D. W., and J. A. Zeh. 2000. "Reproductive Mode and Speciation: The Viviparity-Driven Conflict Hypothesis." *BioEssays* 22: 938–946.

Supporting Information

Additional supporting information can be found online in the Supporting Information section. **Data S1:** mec70409-sup-0001-DataS1.docx.**Methods S1**. Description of the approach used for demultiplexing, filtering and assembly of raw reads. **Table S1:** Sampled locations of 14 populations of *Dianthus rupicola*. **Table S2:**. Akaike information criterion (AIC) scores and ΔAIC scores (relative to best model) for each candidate demographic model conducted on two *Dianthus rupicola* ecotypes. In bold the best-fit demographic model. **Figure S1:** Candidate demographic scenarios for two *Dianthus rupicola* ecotypes. Red denotes the *rupicola* ecotype (RUPI) and blue denotes the *aeolicus* ecotype (AEOL). Models testing for the presence of migration are denoted by two-headed arrows representing bidirectional migration events (m; scenario 2, 4, 6, 8, 10). Potential bottlenecks during divergence were tested in scenario 3, 4, 7, 8. The best model is indicated by black borders. **Figure S2:** Phenotypic differentiation among *Dianthus rupicola* individuals from two ecotypes. Principal component analysis (PCA) (A) and Linear Discriminant Analysis (LDA) (B) on phenotypic traits. Red denotes the *rupicola* ecotype (RUPI) and blue denotes the *aeolicus* ecotype (AEOL). **Figure S3:** Inter-ecotype reciprocal crosses in *Dianthus rupicola*. Seed development was observed at 9 days after pollination. Cross combinations are presented as pollen donor × seed parent. Red denotes the *rupicola* ecotype (RUPI) and blue denotes the *aeolicus* ecotype (AEOL). **Figure S4:** Estimation of the optimal number of ancestral populations for 62 individuals of *Dianthus rupicola* according to the cross-entropy criterion. **Figure S5:** Admixture proportions for $K = 2$–10 for 62 individuals of *Dianthus rupicola*.